

## Spectroscopy of Radioactive Beams from Single-Nucleon Knockout Reactions: Application to the *sd* Shell Nuclei $^{25}\text{Al}$ and $^{26,27,28}\text{P}$

A. Navin,<sup>1,2</sup> D. Bazin,<sup>1</sup> B. A. Brown,<sup>1,3</sup> B. Davids,<sup>1,3</sup> G. Gervais,<sup>1,3,\*</sup> T. Glasmacher,<sup>1,3</sup> K. Govaert,<sup>1</sup> P. G. Hansen,<sup>1,3</sup>  
M. Hellström,<sup>4</sup> R. W. Ibbotson,<sup>1</sup> V. Maddalena,<sup>1,3</sup> B. Pritychenko,<sup>1,3</sup> H. Scheit,<sup>1,3</sup> B. M. Sherrill,<sup>1,3</sup> M. Steiner,<sup>1</sup>  
J. A. Tostevin,<sup>5</sup> and J. Yurkon<sup>1</sup>

<sup>1</sup>*National Superconducting Cyclotron Laboratory, Michigan State University, East Lansing, Michigan 48824*

<sup>2</sup>*Nuclear Physics Division, Bhabha Atomic Research Centre, Trombay, Mumbai 400 085, India*

<sup>3</sup>*Department of Physics and Astronomy, Michigan State University, East Lansing, Michigan 48824*

<sup>4</sup>*Department of Physics, University of Lund, Lund, P.O. Box 118 S-22100, Sweden*

<sup>5</sup>*Department of Physics, University of Surrey, Guildford, Surrey, GU2 5XH, United Kingdom*

(Received 10 August 1998)

Measurements of deexcitation  $\gamma$  rays in coincidence with the momentum distribution of the projectile residues produced in reactions of the type  $^9\text{Be}(^{28}\text{P}, ^{27}\text{Si} + \gamma)X$  at energies around 65 MeV/u are used to study single-nucleon stripping to individual states. The cross sections are compared with calculations based on an eikonal model description of the reaction and the shell model. The measurements indicate that the halo character of the ground state and other detailed spectroscopic information can be derived using knockout reactions in inverse kinematics. [S0031-9007(98)07825-9]

PACS numbers: 25.60.Gc, 21.10.Jx, 25.70.Mn, 27.30.+t

A new and general method applicable to nuclear spectroscopy of radioactive beams is presented. The method is based on obtaining partial cross sections from the measured  $\gamma$ -ray intensities (identifying the individual final states) arising from the decay of states populated in the projectile residue in single-nucleon removal reactions. An extension [1] of the eikonal model is used for translating the measured cross sections into spectroscopic factors. A signature of the orbital angular momentum involved in the reaction is provided by the longitudinal momentum distribution of the projectile residue observed in coincidence with the deexcitation  $\gamma$  rays.

Direct nuclear reactions [2] have for many years been one of the most powerful tools for the study of nuclear structure. The current experiment is a variation on this theme. Momentum wave functions of bound fermions in atomic and nuclear systems have been obtained using  $(e, 2e)$ ,  $(p, 2p)$ , and  $(e, e'p)$  reactions [3]. Studies using electrons are not yet possible with radioactive beams. The advantages of the technique described in this article relate to the large nucleon-knockout cross sections. The technique is applicable at energies greater than approximately 50 MeV/u, characteristic of radioactive beams produced in projectile fragmentation [4,5]. Transfer reactions can provide equivalent information, but at energies above 20 MeV/u the proton angular distributions lose most of their characteristic  $l$  dependence and the magnitudes of the cross sections drop sharply with increasing energy [2,6]. These  $(d, p)$  reactions, also performed in inverse kinematics, require targets more than an order of magnitude thinner than for the technique described here and the identification of the states in the residual nuclei is limited by the energy and angular resolution of the proton detectors [7].

The narrow momentum distribution of the projectile residue associated with the stripping of a halo nucleon is a direct measure of the large spatial extent of the wave function [8]. A closer analysis [9] shows that these measurements are insensitive to the part of the wave function lying in the shadow of the projectile core. In the present work we extend the observations to more deeply bound states in the projectile residue. The observed momentum distributions then reflect essentially the momentum content on the nuclear surface [10] and the analysis requires a more detailed treatment of the target-core interpenetration [1].

The present work is motivated by a search for changes in nuclear structure in the *sd* shell due to the predicted existence of proton halos in the nuclei  $^{26,27,28}\text{P}$  [11]. These isotopes have proton separation energies of 0.14(20), 0.897(35), and 2.066(4) MeV, respectively. The phosphorus isotopes are the lightest nuclei expected to have a ground state with a dominant contribution of a  $\pi s_{1/2}$  orbital. The halo character is expected to manifest itself through relatively large stripping cross sections and narrow longitudinal momentum distributions. The shell-model structure and properties of these nuclei have been discussed in a recent paper [11]. Large halos, strictly speaking, are possible only for neutrons in *s* and *p* states, and the effect of the Coulomb barrier will always make a proton halo less extended [12]. Even in the limit of zero binding energy the halo is of finite size. Because of the effect of the Coulomb barrier, the proton halo for an *s* state and a core charge of 14 is expected to be of relatively modest size compared with the corresponding neutron case. The present measurements were extended to include  $^{25}\text{Al}$  ( $S_p = 2.27$  MeV) for a comparative study of proton removal from a nucleus differing only by a few

nucleons from the phosphorus isotopes but expected to have a negligible  $\pi s_{1/2}$  component [13].

Radioactive beams of  $^{25}\text{Al}$  and  $^{26,27,28}\text{P}$  with energies of approximately 65 MeV/u and momentum spreads of 0.5% were produced in fragmentation reactions using a 100 MeV/u  $^{36}\text{Ar}$  beam on a 470 mg/cm<sup>2</sup> Be target and were purified using the A1200 fragment separator at the National Superconducting Cyclotron Laboratory (NSCL) [14]. The large acceptance S800 superconducting spectrograph [15], operated in a dispersion-matched mode, in conjunction with the focal plane detector setup were used to identify and measure the momentum distributions of the projectile residues produced in one-proton breakup reactions of the radioactive beams on a 14 mg/cm<sup>2</sup> Be target. Time-of-flight information over a distance of 70 m along with energy measurements obtained with a segmented ion chamber and a 5 cm thick plastic scintillator were used to identify and measure the yields of the fragments in the reaction. Two  $x/y$  position-sensitive cathode-readout drift chambers recorded the momentum and angle information of the fragments at the focal plane of the spectrograph. The momentum and scattering angle of the fragments after the reaction were then reconstructed from the known magnetic field and positions at the focal plane using the ion optics code COSY [16]. The measured parallel momentum distributions for  $^{25}\text{Al}$  and the  $^{26,27,28}\text{P}$  isotopes are shown in Fig. 1. Only statistical errors are shown.

The  $\gamma$  rays in coincidence with the breakup events were measured using the NSCL position-sensitive NaI(Tl) array of 38 detectors [17] placed around the target chamber. The  $\gamma$ -ray spectra obtained in coincidence with  $^{24}\text{Mg}$  and  $^{27}\text{Si}$  projectile residues are shown in Fig. 2. With the limited  $\gamma$ -ray data it was not possible to construct a complete input-output balance for each level. We have instead used known [18] level schemes and branching ratios together with the theoretical direct cross sections to construct the indirect feeding. The example of  $^{28}\text{P}$  is shown in Fig. 3.

The theoretical nucleon-knockout cross section leading to a given final state  $n$  (parity and angular-momentum quantum numbers are implicit in our notation) can be written as a sum over the allowed angular-momentum transfers  $j$

$$\sigma(n) = \sum_j C^2 S(j, n) \sigma_{sp}(j, B_n). \quad (1)$$

Each term in the sum in Eq. (1) is a product of two factors.  $C^2 S(j, n)$ , the spectroscopic factor of the removed nucleon with respect to a given core state, is calculated from the shell model [19] and accounts for the intrinsic structure. The reaction factor  $\sigma_{sp}(j, B_n)$ , the cross section for the removal of a nucleon from a single-particle state with total angular momentum  $j$ , is calculated in the eikonal model. The assumed nucleon separation energy  $B_n$  is the sum of the nucleon separation energy for the projectile and the excitation energy of the state  $n$ .

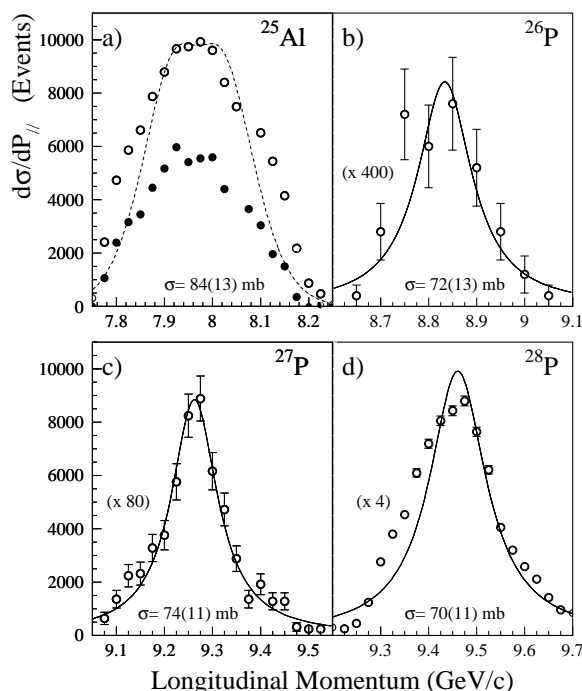


FIG. 1. Longitudinal momentum distributions, in the laboratory frame, of the projectile residue formed in a one-proton removal reaction. The integrated total cross sections are indicated. (a) ( $^{25}\text{Al}$ ,  $^{24}\text{Mg}$ ): the open (filled) circles are the distribution without (with) a coincident  $\gamma$  ray from the  $2^+ \rightarrow 0^+$  transition in  $^{24}\text{Mg}$ . The dotted line corresponds to a calculated momentum spectrum for an  $l = 2$  proton, using a black disk model (see text). The corresponding width is 265 MeV/c. (b)–(d) ( $^{26,27,28}\text{P}$ ,  $^{25,26,27}\text{Si}$ ): the continuous lines represent Lorentzian fits. The corresponding widths are 137(33), 116(8), and 143(14) MeV/c, respectively.

The single-particle cross sections entering Eq. (1) have been calculated by Tostevin [1], who extended the methods of [20] to estimate the required integrated partial cross sections. Expressed in terms of the profile functions  $S_C$  and  $S_N$  for the core ( $C$ ) and nucleon ( $N$ ) interactions with the target, the probability of stripping [21] becomes

$$P(n) = \langle \phi_{IM} | (1 - |S_N|^2) |S_C|^2 | \phi_{IM} \rangle, \quad (2)$$

where the wave function is that of the initial ( $C + N$ ) state. The single-particle cross section is obtained by integrating over the impact parameter and averaging over  $M$  states. This expression has an intuitively simple interpretation: the first factor represents the probability that the nucleon interacts with the target and the second factor is the associated probability that there be no interaction between the core and the target. The additional contribution to the one-nucleon removal cross section arising from diffractive dissociation was also included [1]. For halo states this is of comparable magnitude, but it becomes considerably smaller for states with higher angular momentum or binding energy. The profile functions were calculated using a parametrized nucleon-nucleon interaction [1] and Gaussian core and target densities consistent with electron scattering data.

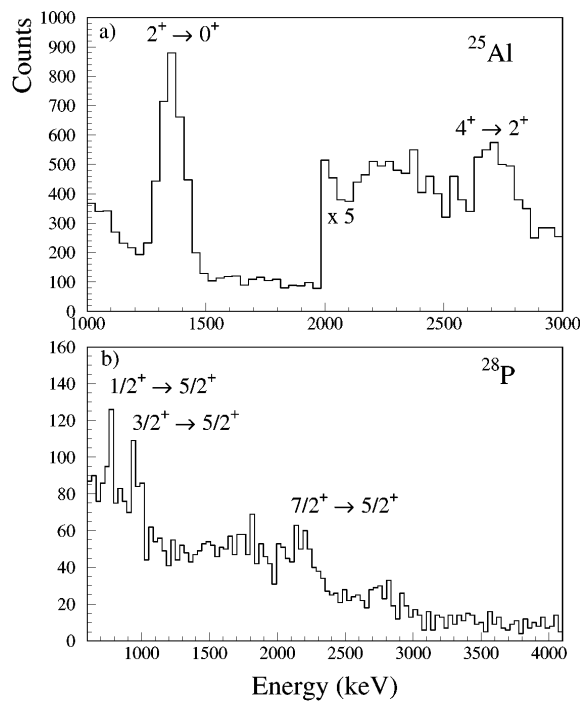


FIG. 2. Doppler corrected  $\gamma$ -ray spectra obtained in coincidence with the residues (a)  $^{24}\text{Mg}$  and (b)  $^{27}\text{Si}$ . The broad peak at around 2.1 MeV in (b) could have contributions from several unresolved transitions.

The longitudinal momentum distributions were calculated in an extension of a model [9] that replaces the profile functions by a sharp cutoff (black disk) approximation. The cutoff radii were chosen to reproduce the core-target and nucleon-target total cross sections, and it was verified that with this choice, the stripping cross sections and their dependence on the separation energy agree approximately with those calculated in [1]. The momentum distribution is obtained as the spatial integral of the one-dimensional Wigner function. In the earlier calculation the wave function was approximated by its value along the trajectory of the target; in the present work the full three-dimensional integration was carried out. This modification has an appreciable effect on the cross section for deeply bound states or for a charged valence nucleon, but it is less important for the width of the momentum distribution.

Figure 1 clearly illustrates the variance in the shapes of the longitudinal momentum distributions for  $^{25}\text{Al}$  as compared to the phosphorus isotopes. For  $^{25}\text{Al}$ , the longitudinal momentum spectra as seen from Fig. 1a have the same  $d$ -wave shape for the ground and excited states. The dominance of  $d$ -wave removal is predicted by theory [13,19] and leads to the following cross sections in mb with the experimental values given in brackets: total, 47 [84(13)];  $4^+ \rightarrow 2^+$ , 9[8(4)];  $2^+ \rightarrow 0^+$ , 36 [42(10)]. The excited states in this case are mainly fed indirectly, i.e., via unobserved higher states. The difference between the measured and calculated total cross section is not yet understood. The total cross sections are 62 [72(13)],

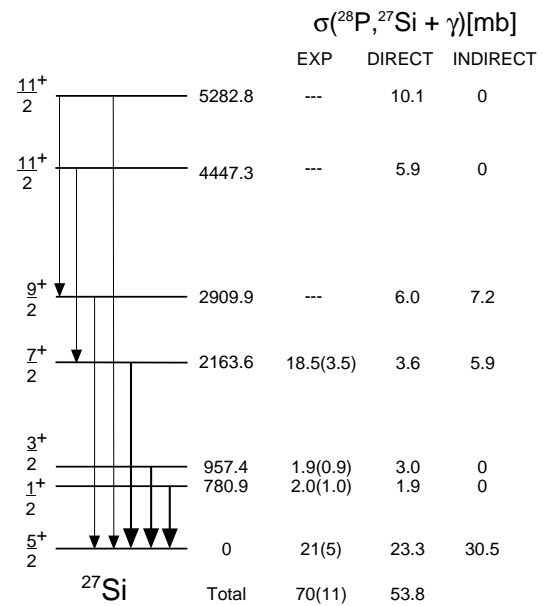


FIG. 3. Simplified level scheme for the  $^{27}\text{Si}$  core based on [18]. The observed  $\gamma$  rays are shown as thickened arrows and the experimental cross sections include both direct and indirect contributions. The calculated partial cross sections are given alongside. The indirect feedings are obtained from the calculated direct feeding of the higher lying states and the known  $\gamma$ -ray branchings. The measured experimental cross section for the *direct* population of the ground state is obtained from the analysis of the momentum spectrum in Fig. 4b. The cross section for the 2164 keV level may include contributions from unresolved transitions.

82 [74(11)], and 54 [70(11)] for the  $^{26,27,28}\text{P}$  isotopes, respectively. The ground state spin for  $^{26}\text{P}$  was assumed to be  $3^+$  [11]. A calculation assuming a spin of  $1^+$  would give a cross section of 36 mb with a negligible  $s$ -wave contribution inconsistent with the measurement.

The expected  $s$  character for the valence proton of the phosphorus isotopes lends special interest to the reactions leading to the Si ground states and can be extracted from the momentum distributions measured with and without  $\gamma$  rays in coincidence. Because of the low statistics of the  $\gamma$  spectra, the analysis was performed by tagging the momentum distributions with any coincident  $\gamma$  event greater than 0.25 MeV. The longitudinal momentum distribution of the  $^{27}\text{Si}$  residues observed in coincidence and anticoincidence with  $\gamma$  rays is shown in Fig. 4a. The finite efficiency for the detection of the  $\gamma$  rays implies that the anticoincidence spectrum represents an admixture of both ground and excited components. These, shown in Fig. 4b, were extracted as a linear combination of the two spectra of Fig. 4a using estimates of a total  $\gamma$ -ray efficiency of 54(5)% (including the effect of  $\gamma$ -ray cascades) and a 10(5)% probability for a coincidence with a background event, i.e., a neutron or a  $\gamma$  ray from the target. The shapes of the extracted momentum distribution corresponding to the ground state transition and the sum of all transitions to excited states are characteristic of essentially pure  $l = 0$

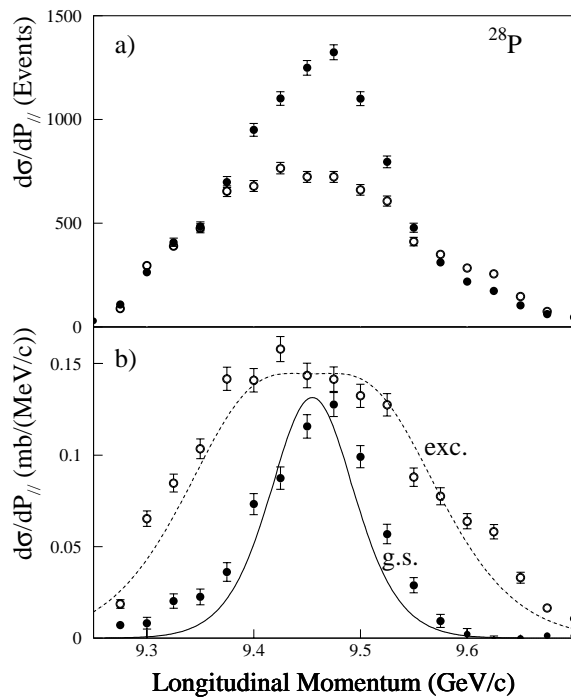


FIG. 4. Longitudinal momentum spectra for  $^{27}\text{Si}$  projectile residues. (a) The (filled) open circles correspond to the absence (presence) of coincident  $\gamma$  rays in the NaI(Tl) array. (b) Derived longitudinal momentum spectrum corresponding to the ground (filled) and excited (open) states in the projectile residue  $^{27}\text{Si}$  obtained from Fig. 4a. The continuous and dashed lines are the calculated longitudinal momentum distributions for the  $s$  and  $d$  states, respectively. The widths are 93 and 248 MeV/ $c$  in the laboratory frame.

and  $l = 2$  components, respectively, as can be seen from the theoretical curves. Similar results were obtained for the case of  $^{26,27}\text{P}$ . The measured gross momentum distributions in Figs. 1b–1d are thus clearly a mixture of  $s$  and  $d$  components and hence of limited significance. The measured branching ratios of 55(17), 30(10), and 30(6)% combined with the measured total cross section giving ground state cross sections of 40(14), 22(8), and 21(5) mb for  $^{26,27,28}\text{P}$ , respectively. These are in good agreement with the theoretical direct ground state components of 36, 23, and 23 mb. The good agreement between the calculated and measured momentum distribution corresponding to the ground and excited states and also the measured cross sections confirm the shell-model predictions that the ground states have a dominant  $s$  component whereas the excited states involve  $d$  components. These large cross sections and narrow momentum widths for the ground state transition are evidence for the proton halo structure discussed in [11].

In summary, a new method for extracting spectroscopic information in experiments using fast radioactive beams has been reported. Its application to several cases in the  $sd$  shell demonstrates that valuable nuclear-structure and angular-momentum information can be obtained from measurements of partial cross sections and momentum dis-

tributions in single-nucleon removal reactions. The important role of the  $\pi s_{1/2}$  orbital in the predicted halo structure of the neutron-deficient phosphorus isotopes has been confirmed. At present, intensity and  $\gamma$ -ray resolution seriously limit the technique, but the higher beam intensities and improved detection techniques expected to be available within the next few years will offer interesting possibilities for studying nuclei far from the valley of stability.

This work was supported by NSF Grants No. PHY-9528844 and No. PHY-9605207.

\*Present address: Physics Division, Argonne National Laboratory, Argonne, IL 60439.

- [1] J. A. Tostevin, in Proceedings of the Nuclear Structure at the Extremes, Lewes, United Kingdom, 1998 [J. Phys. G (to be published)].
- [2] G. R. Satchler, *Direct Nuclear Reactions* (Oxford Univ. Press, New York, 1991).
- [3] G. Jacob and Th. A. Maris, Rev. Mod. Phys. **38**, 121 (1966); I. E. McCarthy and E. Weigold, Rep. Prog. Phys. **51**, 299 (1988); V. R. Pandharipande, I. Sick, and P. K. A. deWitt Huberts, Rev. Mod. Phys. **69**, 981 (1997).
- [4] H. Geissel, G. Münzenberg, and K. Riisager, Annu. Rev. Nucl. Part. Sci. **45**, 163 (1995); D. J. Morrissey in Ref. [5], p. 337.
- [5] *International School of Heavy-Ion Physics, 4th Course: Exotic Nuclei*, edited by R. A. Broglia and P. G. Hansen (World Scientific, Singapore, 1998).
- [6] J. S. Winfield *et al.*, Phys. Lett. B **203**, 345 (1988).
- [7] S. Fortier *et al.*, in Proceedings of the 2nd International Conference on Exotic Nuclei and Atomic Masses (ENAM), Bellaire, 1998, edited by B. Sherrill (to be published).
- [8] N. A. Orr *et al.*, Phys. Rev. Lett. **69**, 2050 (1992); J. H. Kelley *et al.*, Phys. Rev. Lett. **77**, 5020 (1996).
- [9] P. G. Hansen, Phys. Rev. Lett. **77**, 1016 (1996).
- [10] J. Hufner and M. C. Nemes, Phys. Rev. C **23**, 2538 (1981).
- [11] B. A. Brown and P. G. Hansen, Phys. Lett. B **381**, 391 (1996).
- [12] K. Riisager *et al.*, Nucl. Phys. A **548**, 393 (1992).
- [13] B. H. Wildenthal and B. A. Brown (unpublished).
- [14] B. M. Sherrill *et al.*, Nucl. Instrum. Methods Phys. Res., Sect. B **70**, 298 (1992).
- [15] B. M. Sherrill *et al.* (to be published); J. Yurkon *et al.*, Nucl. Instrum. Methods Phys. Res., Sect. A (to be published).
- [16] M. Berz *et al.*, Phys. Rev. C **47**, 537 (1993).
- [17] H. Scheit *et al.*, Nucl. Instrum. Methods Phys. Res., Sect. A (to be published); R. W. Ibbotson *et al.*, Phys. Rev. Lett. **80**, 2081 (1998).
- [18] P. M. Endt, Nucl. Phys. A **521**, 1 (1990).
- [19] B. A. Brown and B. H. Wildenthal, Annu. Rev. Nucl. Part. Sci. **38**, 29 (1988).
- [20] F. Barranco, E. Vigezzi, and R. A. Broglia, Z. Phys. A **356**, 45 (1996); K. Hencken, G. Bertsch, and H. Esbensen, Phys. Rev. C **54**, 3043 (1996), and references therein.
- [21] The word “stripping” is here used in the sense in which it was coined to describe the breakup of 90 MeV/ $u$  deuterons; see the comment by R. Serber, Annu. Rev. Nucl. Part. Sci. **44**, 1 (1994).